Analysis of a New Multi-Oscillated Current Resonant Type DC-DC Converter

Osamu MATSUO[†]   Hirofumi MATSUO[†]   Yoichi ISHIZUKA[†]   Hiroyuki OTA[‡] †Graduate School of
Science and Technology, Nagasaki University,1-14, Bunkyo-machi, Nagasaki, 852-8521 Japan
‡Fuji Electric Device Technology Co., Ltd. 4-18-1 Tsukama, Matsumoto-shi, Nagano-ken, 565-0456 Japan
E-mail:[†] osamu_matsuo@yahoo.co.jp, [‡] oota-hiroyuki@fujielectric.co.jp

Abstract- **This paper presents the analysis of a new multi-oscillated current resonant type DC-DC converter. Current resonant converters have several remarkable features such as high efficiency, small size, low cost and low noise, and are frequently employed in many portable electronic systems such as personal computers, cellular phones and flat panel displays.**

The current resonant type converter generally employs pulse frequency modulation for constant voltage control in the output. For this reason, the magnetizing current through the converter not only causes a power loss under a light load, but also a loss during stand-by.

Therefore, this type of converter has a problem in that the required smaller size cannot be achieved, because an auxiliary source is necessary for stand-by.

In order to solve these problems, a new current resonant type power supply is proposed in which two driving methods are employed. In these driving methods, one MOSFET as a main switch is driven by an auxiliary winding of the transformer and another MOSFET as a main switch is driven by the driving IC with a low withstand voltage.

Good agreement of the observed and simulated waveforms was confirmed. In addition, eight distinct states and four distinct operating modes, which compose of the sequence of states, were clarified by experimental and simulated analysis.

Key terms - Multi-oscillated, Current resonant DC-DC Converter, ZCS, ZVS

I. INTRODUCTION

A switching power supply system is required for high efficiency, small size, low noise and low cost, in many areas of portable electronics systems such as personal computers, cellular phones and flat panel displays. Current resonant type converters in switching power systems have generally employed pulse frequency modulation [1],[2].

However, this type of converter has problems, in which a magnetizing current through the converter causes a loss of power under a light load and at stand-by.

For this reason, the small size required for this type of converter cannot be achieved, because an auxiliary source is necessary at standing-by. To solve these problems, a multi-oscillated converter is proposed [3]-[5].

In this paper, a new current resonant type power supply system is devised in which two driving methods are employed. In these driving methods, one MOSFET Q_2 as a high-side main switch is driven by an auxiliary winding of the transformer and another MOSFET Q_1 as a low-side main switch is driven by the driving IC with a low withstand voltage. The experiment results agree well with simulated results.

II. CIRCUIT CONFIGURATION AND OPERATING PRINCIPLE

Figure 1 and 2 show the newly proposed multi-oscillated current resonant DC-DC converter and the timing chart, respectively.
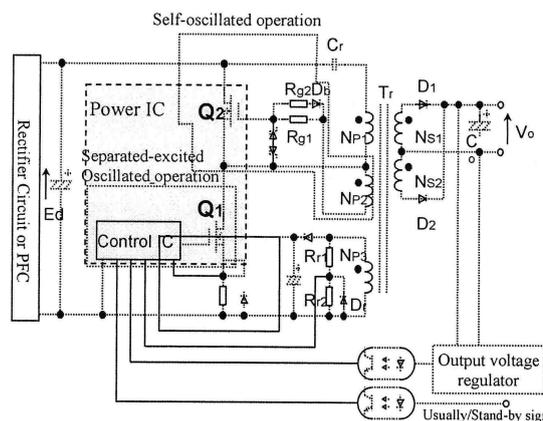
Fig. 1 Proposed multi-oscillated current resonant type DC-DC converter
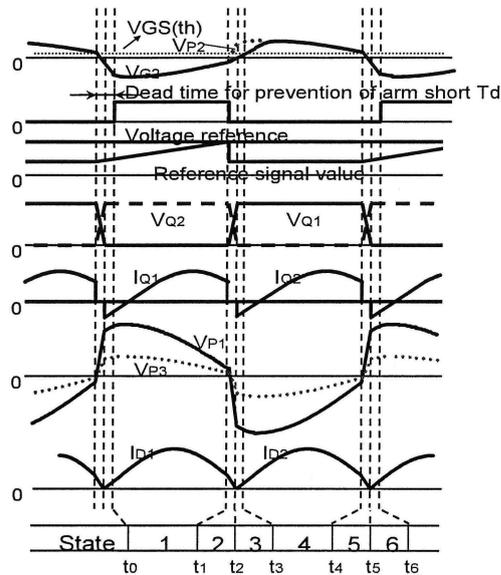
Fig. 2 Timing chart

This converter consists of a half-bridge circuit, which switches Q_1 and Q_2 are operated by a multi-oscillated current resonant driven by an IC with pulse-width modulation (PWM), and an auxiliary winding of the transformer, respectively.

By applying a gate voltage to Q_1 and Q_2 at turn-on and turn-off, switching power losses do not occur due to zero-voltage switching (ZVS) and zero-current switching (ZCS).

In the isolated transformer, the winding N_{P1} is loosely coupled to N_{P1} and N_{S3}, for which the voltage of the leakage inductance is relatively large. Depending on the composition of the resonant circuit with this leakage inductance and the resonant capacitor, the switching power losses of Q_1 and Q_2 are reduced.

The secondary side of the transformer winding is composed of a center-tapped transformer, rectification diodes (D_1 and D_2) that rectify the high frequency AC voltage for the full wave, and an output capacitor (C_o) that smoothes the output voltage.

The control winding (N_{P3}) used to control the supply source is densely coupled to the primary winding (N_{P1}).

The voltage V_{P1} across the primary winding of the transformer is indirectly detected with the voltage across the N_{P3} winding, and is converted to the signal level of the control IC.

The resistors and diode connected between the driving winding N_{P2} and the gate of MOSFET Q_2 prevent the short circuit current from simultaneously passing through Q_1 and Q_2 by varying the gate voltage, slowly at the time of turn-off and at turn-off rapidly.

The output voltage is controlled by feedback, in which the input into the control IC is the voltage command value of the output signal from the output control circuit isolated by a photo coupler.

After the control IC detects the timing for V_{P1} to cross from a negative to positive value, Q_1 is turned on after passing the short-circuit prevention period.

III. ANALYSIS OF STATES AND OPERATING MODES

A. Operating State

In this chapter, the operating modes are analyzed by the simulation and experiment. The following assumptions are made for analysis of the operating modes. Figure 3 shows the equivalent circuit of the converter given in Fig. 1.

(1) The switches (Q_1, Q_2) and diodes behave as ideal switches and diodes.

(2) The transformer winding (N_P, N_S) and inductance (L_r, L_m and L_1) have negligible loss. Also, the transformer core does not saturate, and each inductance is kept constant.

(3) The resonant capacitor (C_r) and the output capacitor (C_o) are zero in the serial equivalent circuit.

(4) The voltage across the output of the PFC is represented as the intermediate voltage E_d.

Furthermore, the capacitor (C_{Q1}-C_{Q2}) and the diodes (D_{Q1}-D_{Q2}) are shown as the output capacitance of Q_1-Q_2 and the body diodes of Q_1-Q_2, respectively.
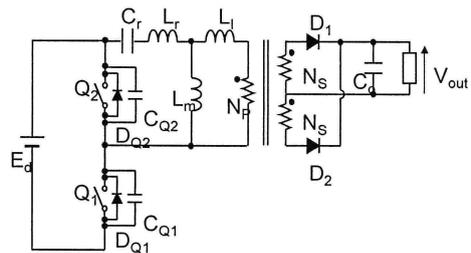
Fig. 3 Equivalent circuit

349

The transformer is dealt with by taking into account the leakage inductance between L_r -L_1 and the magnetizing of L_m. The equivalent circuit given in Fig. 3 is divided into eight behavior states with physical meaning, which are given in Table 1, according to the combination of on and off for Q_1, Q_2, and the diodes D_{Q1}, D_{Q2}, D_1, and D_2.

TABLE 1 States of Behavior

State	Q_1	Q_2	D_{Q1}	D_{Q2}	D_1	D_2
1	on	off	off	off	on	off
2	off	off	off	off	on	off
3	off	off	off	on	off	on
4	off	on	off	off	off	on
5	off	off	off	off	off	on
6	off	off	on	off	on	off
7	off	on	off	off	off	off
8	on	off	off	off	off	off

TABLE 2 Operation Modes

Mode	State sequence
I	$1 \rightarrow 2 \rightarrow 7 \rightarrow 5 \rightarrow 6$
II	$1 \rightarrow 2 \rightarrow 4 \rightarrow 7 \rightarrow 5 \rightarrow 6$
III	$1 \rightarrow 2 \rightarrow 3 \rightarrow 4 \rightarrow 5 \rightarrow 6$
IV	$1 \rightarrow 8 \rightarrow 2 \rightarrow 3 \rightarrow 4 \rightarrow 5 \rightarrow 6$

Taking into account the combination of the eight states of behavior given in Table 1, they are further divided into four operating modes as given in Table 2.

Figure 4 (a)-4(h) show the current route for each of the operating states. The relations between the time chart (Fig. 2) and the equivalent circuit given in Fig. 4 are explained as follows:

(i) State 1 (t_0-t_1)

In this state, before instant t_0, the switches Q_1 and Q_2 turn on and turn off, respectively. Resonant current flows through the series resonant circuit consisting of the resonant capacitor (C_r), the leakage inductors (L_r and L_1) and the magnetizing inductor (L_m) by resonant operation of the converter between C_r, L_r, L_1 and L_m.

At this time the diode (D_1) of the secondary side conducts the energy transferred to the output side.

As a result, the energy is charged into C_r and is stored into L_r, L_1 and L_m.

(ii) State 2 (t_1-t_2)

The timing of the Q_1 turn-off is obtained when the reference voltage is larger than the command voltage, and the reference voltage signal increases in proportion to the time that the auxiliary winding of the transformer reverses to the positive part.

The voltage command value is determined by feedback of the output voltage error from the secondary winding. In this state, the converter operates resonantly by both the series-parallel resonant of the capacitors C_{Q1}-C_{Q2}-C_r, and the resultant of the inductor L_r-L_m-L_1, which charges C_{Q1} by the stored energy in L_r-L_1-L_m, and also C_{Q2} is also discharged.

The resonant current I_{cr} is the resultant of current through C_{Q1} and C_{Q2}, and so each current is equal.

Therefore, the voltage build-up rate of Q_1 and the voltage drop rate of Q_2 are suppressed by the discharge speed of C_{Q1}, and the charge speed of C_{Q2}, respectively.

(iii) State 3 (t_2-t_3)

When the voltage across C_{Q1} reaches the output voltage (E_d) of PFC, the body diode (D_{Q2}) conducts and the voltage of Q_2 is clumped at the voltage E_d.

Also, because part of the stored energy in the magnetizing inductance flows reversely through the series resonant circuit, the secondary diode turns on.

Furthermore, in this state, ZVS and ZCS are achieved depending on whether Q_2 is turned on when the current flows through D_{Q2}.

(iv) State 4 (t_3-t_4)

When the voltage V_{P2} across the driving winding of the transformer reverses to the positive part, switch Q_2 is turned on slowly and the current of the primary side flows reversely through the serial resonant circuit, in which the turn-on speed of switching Q_2 is determined by time constant depending on the resistor R_{g1} between the driving winding N_{P2} and the gate of Q_2. The gate voltage V_{G2} is varied by the time constant. As a result, D_2 conducts, the energy is transferred to the output, C_r is simultaneously discharged into L_r, L_m and L_1.

(v) State 5 (t_4-t_5)

When the voltage V_{P3} across the auxiliary winding of the transformer reverses to the positive part, then the timing causes switch Q_2 to turn off and switch Q_1 to turn on. The resonant behavior in this state is in agreement with the behavior in State 2; that is, Q_2 replaces Q_1 and Q_1 replaces Q_2.

(vi) State 6 (t_5-t_6)

The behavior of State 6 is the same as that for State 3, in which replaces Q_2 replaces Q_1, and Q_1 replaces Q_2.

(a) State1   (b) State2   (c) State3   (d) State4

(e) State5   (f) State6   (g) State7   (h) State8
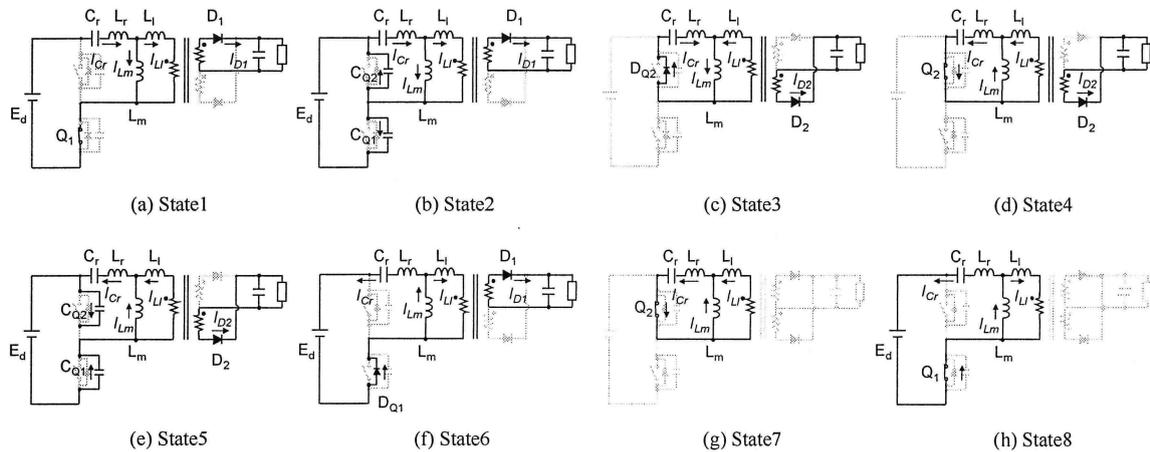
Fig. 4 Equivalent circuit for states of behavior in the converter

(a)   Mode I   (b)   Mode II   (c)   Mode III   (d)   Mode IV
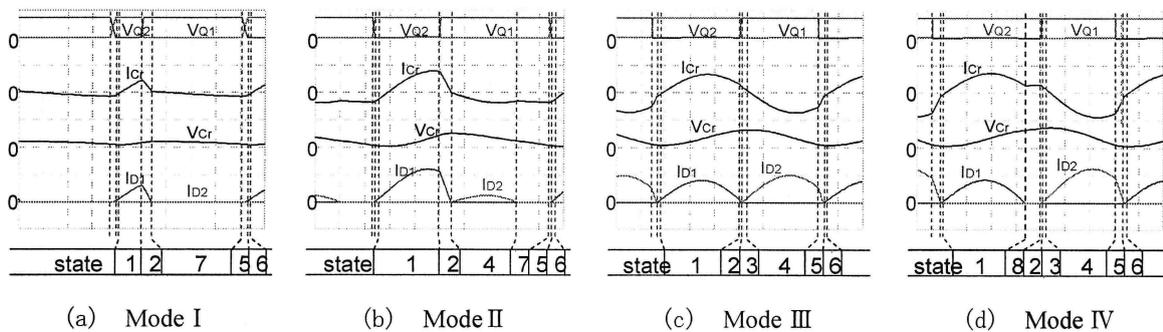
Vertical V_{Q1}, V_{Q2}, V_{cr} :500V/div, I_{Cr} : 2A/div, I_{D1},I_{D2} : 10A/div

Fig. 5 Simulation waveforms

(vii) State 7 (t_6-t_7)

This state appears in both Modes I and II. The energy cannot be discharged to the secondary side, because the stored energy in C_r is small, so that Q_2 turns on. As a result, D_2 is turned off.

(viii) State 8 (t_7-t_8)

This state appears in Mode IV. For the resonant behavior that depends on the resultant of combination of C_r, and L_r, L_m and L_1 due to the large stored energy in C_r, the current flows reversely through the series resonant circuit, and so the circuit takes L_m in reverse bias. As a result, it is the interval for D_1 to turn off, because the energy cannot discharge to the secondary side.

B. Operating Mode

Figure 5 shows the simulated waveforms of the current and voltage for the four operating mode. The conditions for analysis maintain the input voltage at 360 V and the output voltage at 24 V. The operating mode is determined from the voltage amplitude in the secondary side diodes of D_1 and D_2, and the resonant capacitor C_r.

It is found that operating modes appear in the order of I, II, III, IV when the load current is varied from a light load current to the rated load current 6 A and a heavy load current of 7 A.

Operating Mode I and II mainly appear at light loads. The energy in C_r is discharged when the Q_1 switch turns off and Q_2 turns on, and it is charged by applying the output voltage E_d of the PFC when the Q_1 switch turns on.

Therefore, the energy is discharged to the secondary side through the transformer.

However, because the magnetizing inductance L_m is set relatively largely when there is shortage of energy discharged from C_r, operating State 7 appears, in which there is no discharging interval to the secondary side.

As a result, the output current does not flow when operating Mode I appears at light load, but is controlled by being applied only from D_1.

Operating Mode III appears in the vicinity of the rated output. The ripple is reduced and smoothed by the leakage inductance L_1 of the secondary winding and the input capacitor C_o because the current flows continuously through D_1 and D_2. Operating Mode IV appears when the output is larger than the rated output, and when the duty ratio is larger than between 50 % and 60 %.

For the purpose of comparing operating Mode IV with other modes, the voltage amplitude of the resonant capacitor C_r should be considered. Assuming that the voltage amplitude of C_r is equal to the output voltage E_d of the PFC when the maximum output power is applied from C_r in the converter, the maximum output can be approximated by Eq. (1).

$$P(C_r) = C_r \cdot E_d^2 \cdot f_s \qquad (1)$$

where L_r is the resonant frequency, given by

$$f_r = \frac{1}{2\pi\sqrt{C_r \cdot L_r}} \qquad (2)$$

where f_r is the inductance of primary side at the short-circuit of the secondary winding.

Figures 6 and 7 show the voltage amplitude characteristics of the resonant capacitor C_r, and the output current versus voltage for the experiment, respectively.

From Fig. 6, it is found that the operating mode changes with variation in V_{Cr}, and that V_{Cr} is greater than Ed = 360 V at an output current of 7 A.

When V_{Cr} is greater than E_d by varying the output current, State 8 appears, where the power is not applied to the secondary side even when Q_1 turns on.
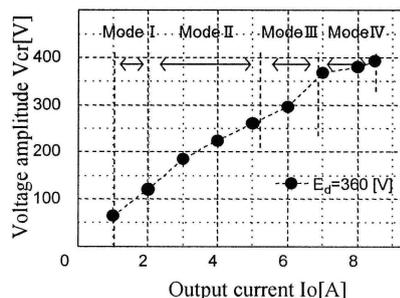
Fig. 6 Voltage amplitude characteristics of resonant capacitor
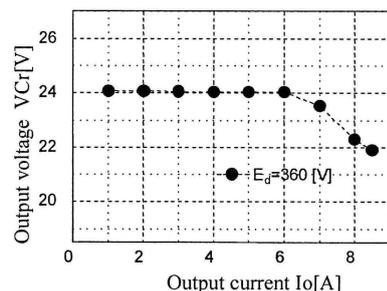
Fig. 7 Output current versus output voltage characteristics

It is for this reason that the operating mode shifts to Mode IV, where the output is smaller than the maximum power. Therefore, it is found that the output voltage is determined by V_{Cr}. This is representative of the new converter.

IV. EXPERIMENT RESULT

In order to verify the operating characteristics the experimental parameters are as follows.

Output voltage E_d of PFC	360 V- 400 V
Output voltage V_o	24 V
Output current of I_o	1 A – 6 A
Winding ratio	
N_{P1}: $N_{S1}(=N_{S2})$; N_{P2}: N_{P3}= 52: 4: 5: 7	
Resonant Capacitor of C_r	22 nF
Resonant inductance of L_r	130 μH
Magnetizing inductance of L_m	1.664 mH
Output Capacitor of C_o	1 mF

Figures 8 and 9 show the frequency operating characteristics and the duty ratio characteristics, respectively. The circuit is controlled by changing the operating frequency at the same time as PWM.

The operating frequency becomes high when the input voltage is high and the load is light. However, the rate of rise is nearly at 24 %.

The reason for this is that the frequency rise is suppressed at a light load, in order to be controlled and dependent on maintaining the duty ratio of the switch Q_2 to be approximately constant.

Figure 10 shows the observed waveforms between a light load and the rated load at an input voltage of 380V.

It is seen that the observed waveforms agree well with the simulated ones. Furthermore, ZVS and ZCS are achieved for the Q_1 and Q_2 switches.

Figure 11 shows the high power efficiency of 94.7 % when the output current varies from 1 A to 6 A.

Fig. 9 Output current versus duty ratio characteristics

(a) At light load(E_d=380V,I_o=1A)   (b) At rated(E_d=380V,I_o=6A)
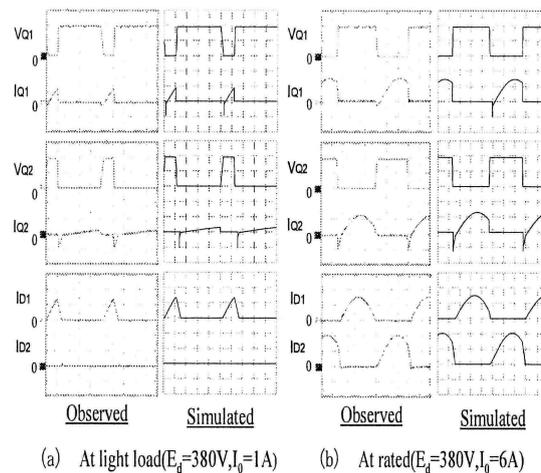
Vertical; VQ1,VQ2 :200V/div, IQ1, IQ2 : 2A/div, IQ1, IQ2 : 5A/div

Fig. 10 Observed waveform

Fig. 8 Output current versus frequency characteristics
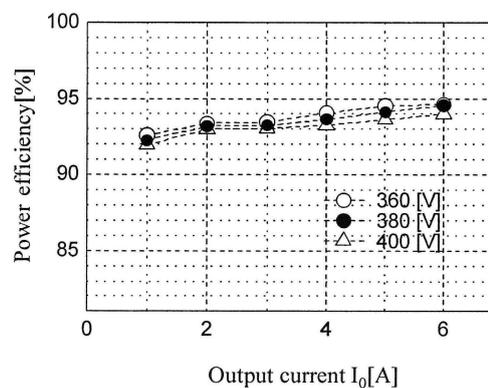
Fig. 11 Output current versus power efficiency

V. CONCLUSIONS

We conclude as follows.

(1) The new converter is controlled by a combination of self-oscillation and a separated oscillation .

(2) This converter has eight states and four operating modes.

(3) When the output power reaches a maximum, the voltage V_{cr} across the resonant capacitor overcomes the voltage E_d from the PFC. As a result, the output voltage decreases.

(4) High power efficiency is obtained at an input voltage 360 V, where 94.7% and 93.4% are achieved at 24V-6A and 24 V-2 A output, respectively.

In order to achieve an improvement of efficiency at light load and minimization of stand-by power at no-load, applications relating to the dependency of the input voltage and load current, and optimization of design for each element, especially the transformer, are currently under study.

The details of these characteristics will be reported in our next paper.

REFERENCES

[1] K. Morita "Novel Ultra Low-noise Soft Switching-mode Power Supply", INTELEC'98, pp.115-122, 1998.

[2] K. Kuwahara, H. Ota "On the Output Increase of a Series Resonant DC-DC Converter", IEICE Technical Report, Vol.105, no.45, EE2005, pp.35-40, 2005

[3] M. Gekinozu, K. Kuroki, K. Mori, T. Fujita "Self-oscillated type current resonant DC/DC converter", IEICE Technical Report, EE99-58, pp.33-38. 2002

[4] Y. Nishikawa, T. Nozawa, S. Igarashi, K. Kuwahara, N. terasawa "Multi-oscillated Current Resonant Converter", Annual Conference Record of EEEJ, Vol.4, pp.157-158, 2002

[5] Y. Nishikawa, T. Nozawa, S. Igarashi, K. Kuwahara, N. Nozawa, H. Ota "A control method that reduce the conversion loss at a light load", Annual Conference of Japan, Industry Application Society, pp.631-632, 2002